PHYSICAL REVIEW LETTERS

Control of Ferromagnetism via Electron Doping in In$_2$O$_3$:Cr

Hannes Raebiger, Stephan Lany, and Alex Zunger

National Renewable Energy Laboratory, Golden, Colorado 80401, USA
(Received 7 March 2008; published 7 July 2008)

Carrier-induced ferromagnetism in wide-gap transparent conductive oxides has been widely discussed and debated, leading to confusion and skepticism regarding whether dilute magnetic oxides exist at all. We show from density-functional calculations within a band-gap corrected approach that ferromagnetic Cr–Cr coupling can be switched on and off via electron doping in the wide-gap transparent *n*-type conductive oxide In$_2$O$_3$. We show that (i) Cr does not produce in In$_2$O$_3$ any free electrons and renders the system an insulating paramagnet. (ii) Extrinsic *n*-type doping of In$_2$O$_3$:Cr via Sn produces free electrons, whose concentration is controllable via the oxygen partial pressure. Such additional carriers stabilize a strong long-range Cr–Cr ferromagnetic coupling.

The prediction of a high Curie temperature in Mn-doped ZnO [1] has set off an avalanche of both experimental and theoretical works following this prediction (see, e.g., Refs. [2–6]) as well as a wide debate on the validity of the above works [7–10]. Interest in 3*d* transition impurities in In$_2$O$_3$ covering the entire row from Sc d^0 to Cu d^8 arose because of the hope of both improving electron conductivity and inducing ferromagnetism. Whereas ferromagnetic signals have been observed in V, Cr, Mn, Fe, Co, and Ni containing In$_2$O$_3$ samples [4,11–18], and theoretically predicted [5,6], more recent experiments have suggested that Cr, Mn, Fe, and Ni in In$_2$O$_3$ are paramagnetic down to cryogenic temperatures [7,10]. Theoretically, ferromagnetic coupling between dilute 3*d* transition impurities (below the bare ion percolation threshold) in oxides has been rationalized by the bound magnetic polaron model [2], which invokes the interaction between the electronic states of the localized 3*d* impurity and those of an extended host structural defect (e.g., oxygen vacancy) leading to an extended hybridized state. However, calculations [8] show that since the oxygen vacancy in such oxides only induces a deep and localized level, the corresponding polaron state cannot lead to extended magnetism. What was not considered, however, is the fact that 3*d* impurities can generally assume different charge states [19], and that the charge state can be controlled by manipulating the Fermi level through doping. This means of Fermi level control is particularly important in oxides like In$_2$O$_3$ or ZnO, in which free-electron concentrations up to 10^{21} cm^{-3} can be achieved via structural defects as well as doping by suitable electron donors, e.g., Sn in In$_2$O$_3$ [20,21]. The possibility of ferromagnetism in oxides due to charged 3*d* transition impurity states has been hardly explored.

In this Letter, we first calculate the range of possible charge states of Cr impurities in In$_2$O$_3$, and determine which charge states correspond to partially occupied gap levels and could lead to ferromagnetism. Finding that none of the charge states of Cr stable within the band gap have

these properties, we study the effect of degenerate *n*-type doping on In$_2$O$_3$:Cr. It is noteworthy that, in predicting the stable Cr charge states within the *entire* band gap, we cannot rely on the standard local density or generalized gradient approximation (GGA) that place the host conduction band too low in energy, contributing to a band-gap underestimation of 2 eV [20]. This unphysical downward sagging of the host conduction band can lead to an incorrect occupancy of 3*d* levels [22,23], which in turn leads to an incorrect description of magnetic 3*d*–3*d* interaction, as discussed below. We therefore employ a host band structure corrected approach [23] to assure a physically correct description of the occupancy of 3*d* levels in In$_2$O$_3$. Second, we use a thermodynamic theory that considers a full range of intrinsic defects in In$_2$O$_3$ as well as the effects of Sn doping, thus realistically predicting the free-electron concentration as a function of growth parameters p_{O_2} and T. This allows us to predict the effect of electron doping on Cr–Cr magnetism. We find that electron doping leads to Cr–Cr ferromagnetism, while nonconductive samples are paramagnetic. We predict the electron concentrations required for optimal ferromagnetic properties.

In order to correct host crystal band structure, we add, within the PAW method [24], nonlocal external potentials $V_{T,\ell}$ to the effective Kohn-Sham potentials, depending on the atom type T and the angular momentum ℓ [23]. The set of potential parameters (given in eV), $V_{In\,s} = 10.5$, $V_{In\,p} = 0$, $V_{O\,s} = -6.4$, and $V_{O\,p} = -2.0$, together with the GGA + U parameters $U_{In\,d} = 5.5$ and $J = 1.0$, are empirically determined such as to fit multiple target band structure properties of the host In$_2$O$_3$ [25]. While these individual parameters are not necessarily unique, they combine to produce a $\vec{k}$-dependent upward shift of the oxide conduction band, mostly achieved by a repulsive potential on the In *s* orbitals. For the Cr impurity, we determined $U_{Cr\,d} = 2.6$ and $J = 1.0$ to reproduce the correct thermochemical stability of CrO$_2$ and Cr$_2$O$_3$, according to Ref. [26]. Total-energy band structure calculations of

In_2O_3 in 80 atom supercells, where one or two In atoms are replaced by a Cr atom, are carried out using the projector augmented-wave method [24] and a $3 \times 3 \times 3$ $\vec{k}$-point sampling mesh.

In the bixbyite structure of In_2O_3 (space group $Ia\bar{3}$), one quarter of the In atoms (Wyckoff position b, denoted α in the following), are located inside an oxygen tetrahedron with equal In–O distances, and three quarters of the In atoms (Wyckoff position d, denoted β), are located inside a more distorted octahedron with three different In–O distances. The isolated Cr^0 shows (center column in Fig. 1) a fully occupied majority spin t_+^3 level in the lower part of the band gap and an empty e_+^0 level resonant slightly above the conduction band minimum E_c. All minority spin levels are unoccupied. Thus, in the t_+^3 configuration each Cr atom induces a net magnetization of 3 Bohr magnetons. The occupied Cr^0 gap levels can be ionized to Cr^+ ($t_+^3 \rightarrow e_+^2 a_+^0$, left column in Fig. 1), giving a deep donor with a transition energy at $\varepsilon(0/+) = E_c - 2.9$ eV in the lower part of the band gap. This is calculated from total-energy differences for charge states q and q' as

$$\varepsilon(q/q') = \frac{E(q) - E(q')}{q - q'} - E_c. \qquad (1)$$

Since $\varepsilon(0/+)$ is far below E_c, ionizing this donor does not occur thermally and requires p-type doping, which is unlikely, as In_2O_3 is naturally n-type even without external doping [20]. Upon degenerate electron doping (e.g., via heavy Sn substitution), however, it is possible to occupy the e_+ resonance inside the conduction band, and form the negatively charged Cr^- state at $\varepsilon(-/0) = E_c + 0.6$ eV ($t_+^3 e_+^0 \rightarrow t_+^3 a_+^1$, right column in Fig. 1). Both positive
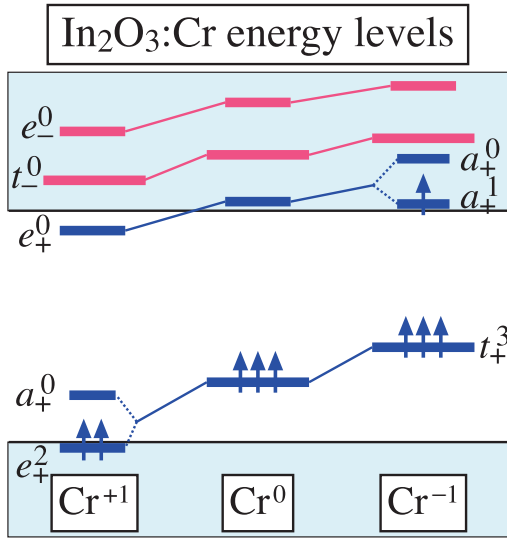
and negative charge states (but not the neutral state) undergo a Jahn-Teller distortion and level splitting shown in Fig. 1.

Partial occupancy of 3d levels can drive ferromagnetism [27], as is illustrated in Figs. 2(a) and 2(b). Here the a levels of two isolated Cr atoms, Cr1 and Cr2 interact and split into bonding (a_b) and antibonding levels (a_a), as seen in the Cr–Cr density of states in Figs. 2(c) and 2(d). Partial occupancy of the isolated Cr a [Fig. 2(a)] leads to preferentially occupying the lower energy bonding level, and thus lowering the total energy, whereas full occupancy of the isolated Cr a [Fig. 2(b)] leads to equal filling of the a_b and a_a levels and thus no energy gain. A similar mechanism was shown to stabilize the ferromagnetic interaction between the partially filled Cr t^1 and Mn t^2 levels in GaAs, whereas fully occupied Fe t^3 (or empty V t^0) levels in GaAs exhibit no ferromagentic coupling [27]. Thus, for the fully occupied Cr t_+^3 levels of the charge neutral Cr^0 in In_2O_3, such a mechanism predicts no energy gain from ferromagnetic coupling. Figure 3 shows our calculated pairwise ferromagnetic stabilization energy

$$\Delta_{FM}(R) = E_{FM}(R) - E_{AF}(R) \qquad (2)$$

as a function of pair distance R, where $E_{FM}(R)$ and $E_{AF}(R)$ are the total energies of ferromagnetic and antiferromagnetic pairs, respectively, with the Cr–Cr distance R of up to 6 Å. As expected from the considerations above, in the absence of external carriers ($n_e = 0$, Fig. 3) Δ_{FM} hardly deviates (within a few meV) from zero, and thus only a

FIG. 1 (color online). Electronic configuration of a single substitutional Cr atom in In_2O_3 in positively charged Cr^{+1}, charge neutral Cr^0, and negatively charged Cr^{-1} state. The shaded areas denote the valence and conduction bands.
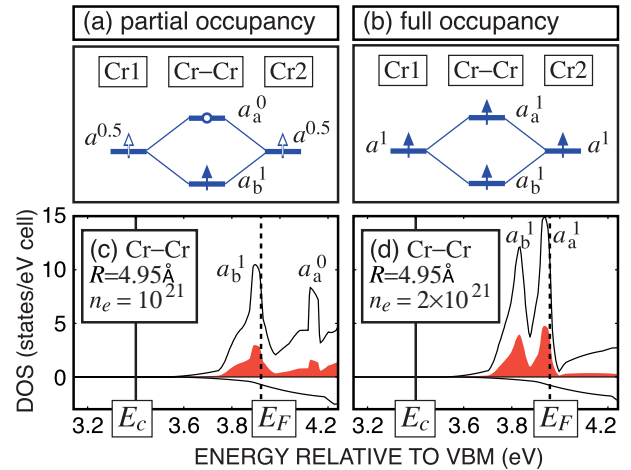

FIG. 2 (color online). Energy level diagram for an interacting Cr–Cr pair formed of atoms Cr1 and Cr2 with (a) partial occupancy stabilizing a ferromagnetic solution and (b) full occupancy giving no energy gain from ferromagnetic coupling. Density of states of an interacting Cr–Cr pair with (c) $n_e = 10^{21}$ cm^{-3} and (d) 2×10^{21} cm^{-3} free-electron carriers. The conduction band minimum E_c and Fermi level E_F are denoted with vertical lines as indicated. The solid line gives the total density of states, and the shaded red (gray) area is the projection on Cr d orbitals.
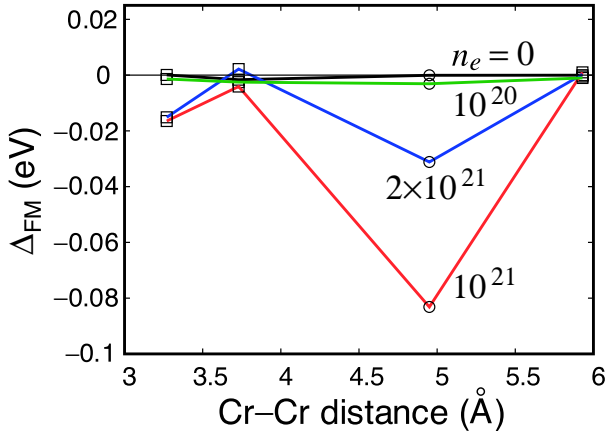
FIG. 3 (color online). Ferromagnetic stabilization energy Δ_{FM} as a function of Cr–Cr distance r. The distance is calculated with the origin the octahedral Cr_α site. The black line denotes Δ_{FM} in the absence of free-carriers (i.e., $n_e = 0$), while the green (light gray), red (gray), and blue (dark gray) lines give Δ_{FM} with free-electron concentrations of $n_e = 10^{20}$, 10^{21}, and 2×10^{21} cm^{-3}, respectively.

paramagnetic response can be expected as indeed is experimentally observed [4,10].

To assess the possibility of ferromagnetism induced by additional n-type doping, we consider the degenerate Sn doping, where E_F can be moved continuously within the conduction band [20]. This leads to partial occupancy of the nondegenerate Cr a level shown in Fig. 2. Next we calculate self-consistently the thermodynamic Fermi level, Cr electronic configuration, and electron concentration from the interplay of electron producers and electron killers [20]. Here, we assume a Cr concentration of 6.25%, a Sn concentration of 3.125%, an equilibrium temperature of $800\,°C$, and the oxygen partial pressure is treated as a variable. We find that even in the presence of 6.25% of Cr, in oxygen-poor conditions (i.e., $p_{O_2} < 10^{-10}$ atm), the free-electron concentration n_e follows closely the tin concentration ($[Sn] = 3.125\% = 10^{21}$ cm^{-3} and $n_e > 0.8 \times 10^{21}$ cm^{-3}). This $n_e \sim 10^{21}$ cm^{-3} indeed leads to the *partially occupied* Cr a resonance inside the conduction band, and roughly corresponds to the Cr electronic configuration $t_+^3 a_+^{0.5} a_+^0$. In an oxygen-rich ($p_{O_2} > 1$ atm) environment, however, interstitial oxygen and indium vacancies form, both of which act as electron-killer defects reducing the free-electron concentration to 3×10^{20} cm^{-3}, leading to a correspondingly lower occupancy of the resonant Cr level.

We proceed by explicitly including the above calculated thermodynamic electron concentrations n_e in our supercell (maintaining a uniform compensating background charge), and calculate the ferromagnetic stabilization energy [Eq. (2)] for different n_e, as shown in Fig. 3. For small free-electron concentrations $n_e \sim 10^{20}$ cm^{-3} no ferromagnetic coupling is observed, but as n_e reaches 10^{21} cm^{-3}——

half-filling the Cr a resonance [28] inside the conduction band shown in Fig. 2(a)—a strong ferromagnetic interaction of $\Delta_{FM} \sim -80$ meV (corresponding roughly to a T_C of ~310 K within a mean field approximation [29,30]) is observed at the rather large Cr–Cr distance of $R = 5$ Å. Further increasing the electron concentration to $n_e = 2 \times 10^{21}$ cm^{-3}, fully occupying the Cr a level, we find a significant decrease in the ferromagnetic stabilization energy, as expected from the model in Fig. 2(b). This mechanism is further confirmed by the densities of states shown in Figs. 2(c) and 2(d), where indeed, the identified a_b and a_a levels are filled as predicted from to the model shown in Figs. 2(a) and 2(b).

The electron-induced ferromagnetic coupling in In_2O_3:Cr is similar to the hole-induced coupling in GaAs:Mn [31], showing a strong directional dependence of Δ_{FM}, as observed also for the Mn–Mn interaction in GaAs:Mn [27]. Like for the Mn–Mn interaction in GaAs:Mn, this directional dependence is of chemical origin, and thus beyond simple RKKY like models. However, unlike Mn in GaAs, Cr in In_2O_3 does not have the dual nature of carrier-producer and magnetic element, and therefore an external electron source is required to produce both charge-carriers and a partially filled Cr a level. Interestingly, even though the Cr a level is rather localized and singly degenerate, it can be partially filled, as under degenerate doping conditions, the resonances in the low (shallow) effective mass conduction band can be filled continuously. In contrast, the heavy valence band mass in GaAs does not allow to move the Fermi level significantly inside the continuum of valence states through acceptor-doping. Therefore partial occupancy of states resonant in the valence band is usually not possible.

Finally, to consider the possibility of magnetism via the bound magnetic polaron model [2], we explicitly include oxygen vacancies in the Δ_{FM} calculation. We find that unlike what has been suggested earlier [4], the oxygen vacancies do not enhance ferromagnetic coupling. Indeed, we calculate that increasing p_{O_2} during growth leads to compensation of the free carriers due to the formation of interstitial oxygen and indium vacancies [20]. This is why experimentally the samples lose their metallicity, and thus also the partial filling of the Cr resonance inside the conduction band, leading to the disappearance of ferromagnetism. The reported tuning of ferromagnetism via modifying oxygen partial pressure during growth [4] supports our model described above. Notice that the free-electron concentration in the ferromagnetic samples is close to half of the Cr concentration—in Ref. [4] the Cr concentration is $2\% = 6 \times 10^{20}$ cm^{-3}, and a high Curie temperature is observed with $n_e = 3 \times 10^{20}$ cm^{-3}. Thus, in the degenerate doping regime the carrier electrons, not depending on their source, cause the partial occupancy of the Cr resonance inside conduction band, leading to ferromagnetism.

To conclude, we have shown, based on a band-gap corrected total-energy functional that In_2O_3 doped with Cr is a ferromagnetic semiconductor, where the ferromagnetism can be turned on and off by tuning the carrier concentration via external doping. As a dielectric insulator, in the absence of free carriers, In_2O_3:Cr is paramagnetic, whereas in the degenerate doping regime, In_2O_3:Cr aligns ferromagnetically. The onset of ferromagnetism occurs as the free-electron concentration reaches half of the Cr concentration. For these Cr and free-electron concentrations a Curie temperature around room temperature could be expected.

[1] T. Dietl, H. Ohno, F. Matsukura, J. Cibert, and D. Ferrand, Science **287,** 1019 (2000).

[2] J. M. D. Coey, M. Venkatesan, and C. B. Fitzgerald, Nat. Mater. **4,** 173 (2005).

[3] K. R. Kittilstved, W. K. Liu, and D. R. Gamelin, Nat. Mater. **5,** 291 (2006).

[4] J. Philip, A. Punnoose, B. I. Kim, K. M. Reddy, S. Layne, J. O. Holmes, B. Satpati, P. R. Leclair, T. S. Santos, and J. S. Moodera, Nat. Mater. **5,** 298 (2006).

[5] A. Gupta, H. Cao, K. Parekh, K. V. Rao, A. R. Raju, and U. V. Waghmare, J. Appl. Phys. **101,** 09N513 (2007).

[6] S. Hu, S. Yan, X. Lin, X. Yao, Y. Chen, G. Liu, and L. Mei, Appl. Phys. Lett. **91,** 262514 (2007).

[7] J. M. D. Coey, Curr. Opin. Solid State Mater. Sci. **10,** 83 (2006).

[8] L.-H. Ye and A. J. Freeman, Phys. Rev. B **73,** 081304(R) (2006).

[9] T. Dietl, T. Andrearczyk, A. Lipińska, M. Kiecana, M. Tay, and Y. Wu, Phys. Rev. B **76,** 155312 (2007).

[10] D. Bérardan, E. Guilmeau, and D. Pelloquin, J. Magn. Magn. Mater. **320,** 983 (2008).

[11] J. He, S. Xu, Y. K. Yoo, Q. Xue, H.-C. Lee, S. Cheng, X.-D. Xiang, G. Dionne, and I. Takeuchi, Appl. Phys. Lett. **86,** 052503 (2005).

[12] Y. K. Yoo, Q. Xue, H.-C. Lee, S. Cheng, X.-D. Xiang, G. Dionne, S. Xu, J. He, Y. S. Chu, S. D. Preite, S. E. Lofland, and I. Takeuchi, Appl. Phys. Lett. **86,** 042506 (2005).

[13] J. Philip, N. Theodoropoulou, G. Berera, J. S. Moodera, and B. Satpati, Appl. Phys. Lett. **85,** 777 (2004).

[14] N. H. Hong, J. Sakai, N. T. Huong, and V. Brizé, Appl. Phys. Lett. **87,** 102505 (2005).

[15] N. H. Hong, J. Sakai, N. T. Huong, and V. Brizé, J. Magn. Magn. Mater. **302,** 228 (2006).

[16] G. Peleckis, X. L. Wang, and S. X. Dou, J. Magn. Magn. Mater. **301,** 308 (2006).

[17] G. Peleckis, X. L. Wang, and S. X. Dou, Appl. Phys. Lett. **88,** 132507 (2006).

[18] P. Kharel, M. B. Sudakar, G. Sahana, R. Suryanarayanan, R. Naik, and V. M. Naik, J. Appl. Phys. **101,** 09H117 (2007).

[19] H. Raebiger, S. Lany, and A. Zunger, Nature (London) **453,** 763 (2008).

[20] S. Lany and A. Zunger, Phys. Rev. Lett. **98,** 045501 (2007).

[21] H. L. Hartnagel, A. L. Dawar, A. K. Jain, and C. Jagadish, *Semiconducting Transparent Thin Films* (Institute of Physics Publishing, Bristol and Philadelphia, 1995).

[22] T. Chanier, M. Sargolzaei, I. Ophale, R. Hayn, and K. Koepernik, Phys. Rev. B **73,** 134418 (2006).

[23] S. Lany, H. Raebiger, and A. Zunger, Phys. Rev. B **77,** 241201(R) (2008).

[24] G. Kresse and D. Joubert, Phys. Rev. B **59,** 1758 (1999).

[25] P. Erhart, A. Klein, R. G. Edgell, and K. Albe, Phys. Rev. B **75,** 153205 (2007).

[26] S. Lany, J. M. Osorio-Guillén, and A. Zunger, Phys. Rev. B **75,** 241203(R) (2007).

[27] P. Mahadevan, A. Zunger, and D. D. Sarma, Phys. Rev. Lett. **93,** 177201 (2004).

[28] The electron doping required to achieve half-filling of the Cr *a* level depends on the relative position of the Cr *a* level with respect to the conduction band. In an uncorrected local density approximation or GGA study, the conduction band is so low in energy that half-filling of the Cr *a* level cannot be achieved under any realistic doping conditions.

[29] H. Raebiger, A. Ayuela, and J. von Boehm, Phys. Rev. B **72,** 014465 (2005).

[30] H. Raebiger, M. Ganchenkova, and J. von Boehm, Appl. Phys. Lett. **89,** 012505 (2006).

[31] H. Ohno, Science **281,** 951 (1998).